Prenatal and early postnatal lead exposure in mice: neuroimaging findings

Diana M. Lindquist[1], Travis Beckwith[1], Kim M. Cecil[1], Francisco Javier Sánchez-Martín[2], Julio Landero-Figueroa[3], Alvaro Puga[2]

[1]Imaging Research Center, Department of Radiology, Cincinnati Children's Hospital Medical Center, Cincinnati, Ohio, USA; [2]Department of Environmental Health and Center for Environmental Genetics, University of Cincinnati College of Medicine, Cincinnati, Ohio, USA; [3]Metallomics Center of the Americas, Department of Chemistry, University of Cincinnati, Cincinnati, Ohio, USA

Correspondence to: Kim M. Cecil, PhD. Department of Radiology, Imaging Research Center, Cincinnati Children's Hospital Medical Center, 3333 Burnet Ave, ML 5033, Cincinnati, OH 45229 USA. Email: kim.cecil@cchmc.org.

Background: Childhood lead exposure has been linked to adult gray matter loss accompanied by changes in myelination and neurochemistry noninvasively revealed by magnetic resonance imaging (MRI) methods. However, the extent, duration and timing of lead exposure required to produce such imaging changes in humans are difficult to ascertain.

Methods: To determine if such changes are related to early exposure to low levels of lead, we treated mouse dams with 0, 3, or 30 ppm of lead acetate in drinking water for 2 months prior to mating through gestation until weaning of the offspring at post-natal day 21. Two male and two female pups from each litter were imaged at post-natal day 60. Volumetric, diffusion tensor imaging and magnetic resonance spectroscopy (MRS) measurements were obtained using a seven Tesla Bruker animal MRI scanner.

Results: Postnatal blood lead levels were identical between groups at the time of imaging. No effects of lead exposure were detected in the volumetric or MRS data. Mean diffusivity in the hippocampus showed significant effects of lead exposure and gender.

Conclusions: These data suggest that low-level, gestational lead exposure in a mouse model produces minimal changes observed by MRI.

Keywords: Lead; magnetic resonance imaging (MRI); magnetic resonance spectroscopy (MRS); diffusion tensor imaging (DTI)

Introduction

Lead is internationally recognized as an environmental hazard associated with cognitive, behavioral, and motor deficits in humans, some of which persist long after exposure to lead has ceased (1-11). These studies, including the Cincinnati Lead Study (CLS), identified compelling evidence that these deficits can result from lead exposure to the developing brain. Debate continues about which periods of development are most vulnerable to the effects of lead and what levels and durations of exposure produce

adverse effects (6). No "minimum safe exposure" has been determined; however, the United Stated Centers for Disease Control recently lowered its reference level to five micrograms per deciliter (μg/dL), the level at which public health actions should be initiated in children of any age.

Neuroimaging studies of adults have associated lead exposure with decreased gray matter volume in brain regions related to executive function and self-regulation (12,13). Further supporting the neurobehavioral evidence that childhood lead exposure during development is

512

Lindquist et al. Neuroimaging early lead exposure in mice

detrimental in the long term, adults from the CLS exposed to lead prenatally and throughout childhood in addition to volume loss (12) displayed altered neuroimaging markers of myelination (14) with patterns of injury and compensation, as well as altered neurochemistry (15). The CLS cohort, with relatively high exposures by comparisons with contemporary levels (mean childhood blood lead level for the CLS cohort approximated 13 µg/dL), was continuously exposed prenatally (maternal blood lead draw at 16 weeks gestation) and throughout childhood from environmental lead residues in their homes and community. Despite extensive lead exposure assessments with blood lead concentrations determined quarterly from birth to 5 years of age and semiannually up to 6.5 years, this rich exposure history still cannot fully address the observed changes to brain volume, neurochemistry, and white matter organization, as cohort members' postnatal child blood lead concentrations are highly correlated (6). Thus, we sought to employ animal models, which allow us to control the extent, duration and timing of lead exposure during development, and to evaluate how specific lead exposure conditions alter neuroimaging outcomes.

The period of embryonic development is the time when the organism is thought to be most sensitive to chemicals and environmental toxins (16). Studies in Wistar rats have shown loss or injury of hippocampal neurons following gestational lead exposure (17,18). Imaging studies of rodents exposed to lead found abnormal increased signal in the hippocampi of adult rats exposed to 1,000 ppm lead acetate from gestation through 90 days compared with controls (17) and increased tissue water diffusivity values in adult Wistar rats after 12 weeks of exposure to 50 ppm lead acetate (19). However, no study to date has conducted a multimodal neuroimaging examination to study the long-term effects on the brains of rodents exposed to lead only during gestation and nursing.

We employed a mouse model with lead exposure throughout gestation, suspended upon weaning at post-natal day 21 (the equivalent of about 12 months in humans). We then determined brain volume with high-resolution anatomical imaging, measured concentrations of select neurochemicals with proton magnetic resonance spectroscopy (MRS) and characterized white matter organization with diffusion tensor imaging (DTI). Both sexes were investigated due to the observed sex-related neuroimaging and behavioral outcomes in humans. We hypothesized that if low-level gestational and early prenatal lead exposure is responsible for changes similar to those

reported in the CLS adults with neuroimaging techniques, then animals exposed to higher doses of lead would have smaller brain volumes, metrics of abnormal white matter, and lower neurochemical concentration levels compared with control animals.

Materials and methods

Animals and lead exposure

C57BL/6 mice (Charles River) were housed in the Vivarium at Cincinnati Children's Hospital Research Foundation housed under standard conditions (10 hours light/14 hours dark) and given ad libitum access to food and water. Female mice were given drinking water containing 0, 3, or 30 ppm lead acetate (Sigma Aldrich, St. Louis, Mo, USA) for a minimum of 2 months prior to mating and were maintained on this water through weaning. Male breeding mice were exposed to leaded water while they were with the females. Pups were weaned at post-natal day 21 and were put on normal water for the duration of the experiment. Drinking patterns and water consumption showed no appreciable differences between the groups. Six litters were used for the 0 ppm group, seven for the 3 ppm group, and eight were used for the 30 ppm group. Generally, one or two mice of each sex from each litter were used, except for the 0 ppm diet where three male mice from each of two litters were used and one group of three females from one litter were used.

Imaging and spectroscopy data acquisition

We obtained anatomical (volumetric) imaging, MRS and DTI data at post-natal day 60 (±1 day). Data were obtained with a Bruker seven Tesla Avance horizontal bore animal magnetic resonance imaging (MRI) system using a 116 mm inner diameter, 400 mT/m gradient insert. Mice were anesthetized and maintained with isoflurane in air to a respiration rate of approximately 120 breaths per minute. The mice were positioned in a custom-built mouse-brain solenoidal coil at magnet isocenter. They were kept warm with a flow of warm air controlled by a thermocouple beneath the mouse, using software from Small Animal Instruments, Inc. (Stony Brook, NY, USA).

After localizer images were acquired, three dimensional (3D) rapid acquisition with relaxation enhancement (RARE) sagittal images were acquired with repetition time/echo time (TR/TE) 1,000/70.56 milliseconds (ms), RARE factor 16, 125 µm × 150 µm × 150 µm resolution, matrix size 256 µm
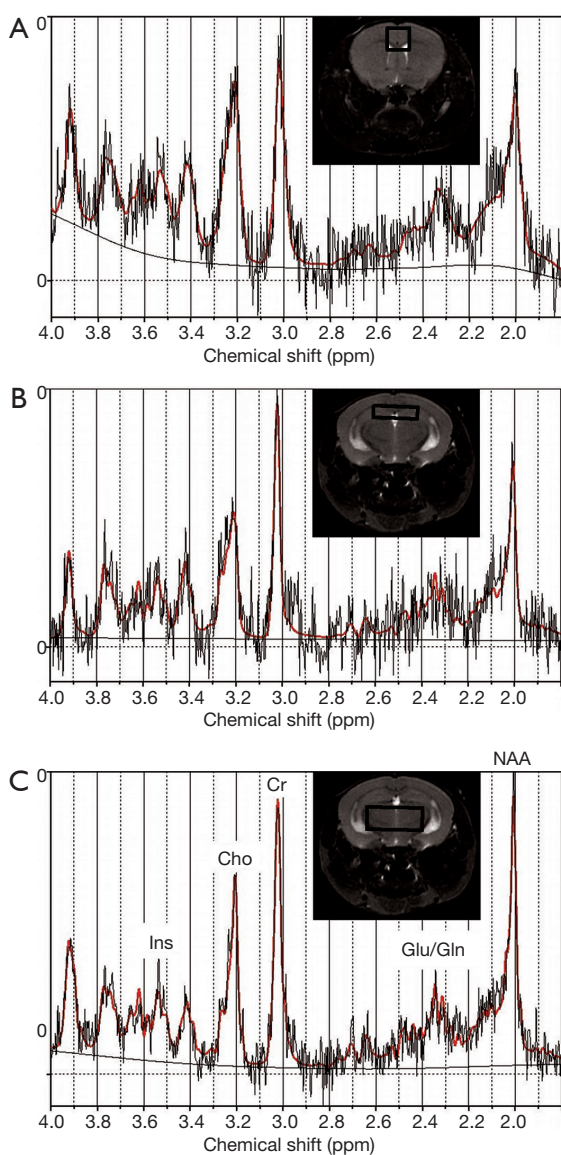
Figure 1 Voxel locations and representative spectrum from cortex (A), hippocampus (B), and thalamus (C). Spectra show the LCModel fit in red over the raw spectrum.

× 128 µm × 128 µm, and respiratory gating; these data were used for volumetric analysis. Single voxel MRS data were acquired in three locations: thalamus [voxel size 5×2×2 mm³, number of averages (NA) = 128], hippocampus (voxel size 4×1×2 mm³, NA =512), and cortex (voxel size 2×2×2 mm³, NA =256) using a point-resolved spectroscopy (PRESS) localization sequence with TR/TE 2,500/20 ms with outer volume signal suppression and variable power radiofrequency pulses and optimized relaxation delays (VAPOR) water suppression. Voxel

locations are shown in *Figure 1*. Reference data without water suppression (NA =4 for each voxel) were also acquired at each location for use in estimating metabolite concentrations. To assess diffusion metrics, diffusion tensor imaging echo planar imaging (DTI-EPI) data were acquired with TR/TE 5,400/40 ms, four shots, 30 directions at a b-value of 670, 75 µm in-plane resolution, matrix 196×168, 700 µm slice thickness, 11 slices and 4 repetitions to cover the brain from the base of the olfactory bulb to the cerebellum. Animals were euthanized after imaging and blood was collected for blood lead analysis and brain tissue was collected for DNA methylation analyses (20).

The numbers of animals are reported for each methodology. Although every mouse underwent the entire protocol, some data were omitted during analysis due to technical artifacts (volumetric and DTI data) or poor spectral quality (MRS).

Data analyses: voxel based morphometry

A total of 65 mice were included in the voxel based morphometry (VBM) analysis: 21 mice (10 female, 11 male) from the 0 ppm group, 22 mice (10 female, 12 male) from the 3 ppm group, and 22 mice (11 female, 11 male) from the 30 ppm group. Volumetric data were cropped to contain the brain and remove non-brain tissue that was contained in the field of view using ImageJ (21). VBM analysis was done in Statistical Parameter Mapping software version 12 (SPM12) (Wellcome Trust Centre for Neuroimaging Functional Imaging Laboratory, http://www.fil.ion.ucl.ac.uk/spm/) using standard procedures (22). Whole brain anatomical images were resized by a factor of 10, imported into SPM12, and manually inspected for artifacts; any images with artifacts were removed from the analysis. The anatomical images were coregistered to a custom gray matter template (22) using SPM12 and then segmented into gray matter (GM), white matter (WM), and cerebrospinal fluid (CSF). GM, WM, and CSF images were manually inspected to ensure proper segmentation. Finally, the segmented images were realigned with the custom template, normalized, modulated, and minimally smoothed by 4 mm. The SPM-reported volumes for each tissue class (GM, WM, CSF) were used to calculate the total brain volume.

Voxel based statistics were conducted using a full factorial analysis in SPM12. F-tests and *t*-tests were run on the smoothed, normalized, modulated GM and WM images with dose, sex, and litter as the factors and brain volume as a covariate. Data were analyzed using the family-wise-error setting with a P value of 0.05.

Table 1 MRS concentration estimates by group and sex: cortex

Metabolite	Female			Male		
	0 ppm	3 ppm	30 ppm	0 ppm	3 ppm	30 ppm
NAA	6.05±0.54 [8]	5.86±0.59 [7]	5.46±1.80 [10]	6.05±0.76 [7]	6.39±0.61 [7]	6.54±0.51 [9]
NAA/Cr	1.02±0.10 [8]	1.06±0.09 [7]	1.02±0.15 [10]	0.97±0.09 [7]	1.03±0.08 [7]	1.06±0.10 [9]
Cr	5.98±0.59 [8]	5.55±0.69 [7]	5.32±1.62 [10]	6.26±0.46 [7]	6.20±0.54 [7]	6.19±0.66 [9]
Cho	1.56±0.20 [8]	1.42±0.23 [7]	1.42±0.43 [10]	1.59±0.16 [7]	1.63±0.14 [7]	1.51±0.15 [9]
Cho/Cr	0.26±0.04 [8]	0.25±0.02 [7]	0.27±0.02 [10]	0.25±0.02 [7]	0.26±0.01 [7]	0.24±0.02 [9]
Ins	4.72±0.96 [8]	4.56±0.61 [7]	4.47±1.65 [10]	4.25±0.85 [7]	4.15±0.42 [7]	4.22±0.90 [9]
Ins/Cr	0.78±0.11 [8]	0.83±0.14 [7]	0.83±0.23 [10]	0.68±0.09 [7]	0.67±0.07 [7]	0.68±0.14 [9]
Glu	7.84±1.15 [8]	8.92±1.00 [7]	8.24±2.76 [10]	8.89±1.32 [7]	9.47±0.85 [7]	9.19±1.28 [9]
Glu/Cr	1.31±0.18 [8]	1.63±0.25 [7]	1.54±0.23 [10]	1.43±0.26 [7]	1.54±0.20 [7]	1.50±0.27 [9]
Gln	5.03±1.22 [8]	5.78±1.50 [4]	4.99±0.65 [7]	4.86±0.84 [7]	4.27±0.92 [5]	4.99±0.54 [7]
Gln/Cr	0.86±0.32 [8]	1.02±0.19 [4]	0.84±0.11 [7]	0.79±0.18 [7]	0.71±0.13 [5]	0.81±0.14 [7]

Values (institutional units) are given as mean ± standard deviation, number of animals in the analysis [n]. MRS, magnetic resonance spectroscopy; NAA, N-acetyl aspartate; Cr, creatine; Cho, choline; Ins, myo-inositol; Glu, glutamate; Gln, glutamine.

Data analyses: MR spectroscopy

Data from a total of 69 mice were retained for the MRS analyses: 21 mice (10 female, 11 male) from the 0 ppm group, 24 mice (10 female, 14 male) from the 3 ppm group, and 24 mice (12 female, 12 male) from the 30 ppm group. MRS data were imported into LCModel (23) for calculation of concentration estimates. Spectra were retained for further analyses if the total signal-to-noise ratio reported by LCModel was greater than or equal to 4 and the Cramer-Rao bounds (a measure of the goodness-of-fit) reported for the metabolites were less than 25%. Sample sizes after removal of spectra not meeting quality threshold are shown with the results in *Tables 1-3*. Concentrations are reported in institutional units.

LCModel concentration estimates were analyzed using ANOVA with dose, sex, and litter as factors using the R package for statistical analysis (www.r-project.org) and corrected for multiple comparisons; P<0.001 was considered significant.

Data analyses: diffusion tensor imaging

A total of 66 mice were included in the DTI analysis: 20 mice (10 female, 10 male) from the 0 ppm group, 22 mice (10 female, 12 male) from the 3 ppm group, and 24 mice (13 female, 11 male) from the 30 ppm group. DTI data were imported into and analyzed with DTIStudio (24) to calculate the fractional anisotropy, radial and axial diffusivity and mean diffusivity. Representative FA maps from three different mice are shown in *Figure 2*. Diffusion metrics

were extracted from regions of interest drawn in the corpus callosum, left and right external capsule, and left and right hippocampus. Results are shown in *Table 4*.

Region-of-interest DTI values for the diffusion metrics were analyzed using ANOVA with dose, sex, and litter as factors using R and corrected for multiple comparisons; P<0.00125 was considered significant.

Results

Blood lead levels

We found no significant difference in blood lead values among the three groups of pups at post-natal day 60. Blood lead levels in pups (n=16 per group) of control, 3 ppm- and 30 ppm-exposed dams were 1.2±1.1, 0.9±0.8 and 1.3± 3.1 µg/dL, respectively, in good agreement with values observed in unexposed mice fed a normal diet (25,26) and consistent with the observations of Virgolini *et al.* (27), who found that blood lead levels normalize roughly 40 days after weaning.

Volumetric measurements

No significant effects of dose, sex, or litter were found.

MRS measurements

Significant effects of sex were found in the thalamus for glutamate (m>f, P=0.00109). No other significant effects were found.

Table 2 MRS concentration estimates by group and sex: thalamus

Metabolite	Female			Male		
	0 ppm	3 ppm	30 ppm	0 ppm	3 ppm	30 ppm
NAA	5.98±0.68 [10]	6.07±0.56 [8]	6.48±2.28 [11]	6.47±0.55 [10]	6.44±0.59 [10]	6.27±0.55 [11]
NAA/Cr	1.06±0.08 [11]	1.11±0.15 [8]	1.10±0.11 [11]	1.09±0.11 [10]	1.11±0.06 [10]	1.14±0.13 [11]
Cr	5.68±0.76 [10]	5.51±0.52 [8]	5.99±2.49 [11]	5.98±0.65 [10]	5.80±0.65 [10]	5.52±0.55 [11]
Cho	1.23±0.19 [10]	1.29±0.13 [8]	1.45±0.43 [11]	1.37±0.12 [10]	1.36±0.20 [10]	1.26±0.19 [11]
Cho/Cr	0.22±0.03 [11]	0.24±0.02 [8]	0.25±0.03 [11]	0.23±0.04 [10]	0.23±0.03 [10]	0.23±0.02 [11]
Ins	3.90±0.75 [10]	4.68±1.21 [8]	4.41±0.67 [10]	4.15±0.83 [10]	3.90±0.51 [10]	4.01±0.96 [11]
Ins/Cr	0.73±0.18 [11]	0.84±0.14 [8]	0.86±0.22 [10]	0.70±0.14 [10]	0.68±0.10 [10]	0.72±0.16 [11]
Glu*	6.69±0.80 [10]	7.40±0.71 [8]	6.75±1.02 [11]	7.61±0.65 [10]	7.83±0.85 [10]	7.43±0.50 [11]
Glu/Cr	1.22±0.21 [11]	1.35±0.18 [8]	1.23±0.31 [11]	1.29±0.22 [10]	1.36±0.13 [10]	1.35±0.14 [11]
Gln	4.21±1.25 [9]	3.87±0.69 [7]	4.34±0.48 [8]	4.26±0.60 [10]	4.52±0.47 [8]	4.24±0.83 [10]
Gln/Cr	0.78±0.33 [10]	0.72±0.16 [7]	0.81±0.08 [8]	0.72±0.14 [10]	0.78±0.12 [8]	0.76±0.16 [10]

Values (institutional units) are given as mean ± standard deviation [n]. *ANOVA revealed an effect of sex with P=0.0011. MRS, magnetic resonance spectroscopy; NAA, N-acetyl aspartate; Cr, creatine; Cho, choline; Ins, myo-inositol; Glu, glutamate; Gln, glutamine.

Table 3 MRS concentration estimates by group and sex: hippocampus

Metabolite	Female			Male		
	0 ppm	3 ppm	30 ppm	0 ppm	3 ppm	30 ppm
NAA	5.66±0.21 [4]	6.28±0.54 [6]	6.03±2.43 [10]	6.59±0.91 [5]	6.31±1.00 [6]	6.62±0.59 [10]
NAA/Cr	0.95±0.09 [4]	0.97±0.09 [6]	1.00±0.07 [10]	0.97±0.04 [5]	0.98±0.08 [6]	1.01±0.12 [10]
Cr	6.03±0.65 [4]	6.48±0.47 [6]	6.17±2.67 [10]	6.77±0.91 [5]	6.46±1.15 [6]	6.62±0.97 [10]
Cho	1.09±0.21 [4]	1.10±0.12 [6]	1.12±0.43 [10]	1.20±0.14 [5]	1.24±0.19 [6]	1.21±0.20 [10]
Cho/Cr	0.18±0.04 [4]	0.17±0.01 [6]	0.19±0.03 [10]	0.18±0.02 [5]	0.19±0.02 [6]	0.18±0.02 [10]
Ins	3.08±1.15 [4]	3.71±0.96 [6]	3.66±1.56 [10]	3.00±0.35 [5]	3.32±0.91 [6]	4.08±1.51 [9]
Ins/Cr	0.50±0.14 [4]	0.57±0.12 [6]	0.67±0.27 [10]	0.45±0.05 [5]	0.53±0.16 [6]	0.59±0.15 [9]
Glu	5.92±0.60 [4]	7.33±1.24 [6]	7.03±2.93 [10]	6.96±1.29 [5]	7.31±1.32 [6]	7.56±1.04 [10]
Glu/Cr	0.98±0.08 [4]	1.13±0.12 [6]	1.14±0.11 [10]	1.02±0.10 [5]	1.16±0.26 [6]	1.16±0.21 [10]
Gln	5.36±1.40 [3]	5.09±0.79 [5]	4.61±0.81 [5]	3.79±0.51 [5]	4.50±0.86 [4]	5.16±0.53 [6]
Gln/Cr	0.86±0.28 [3]	0.79±0.15 [5]	0.71±0.14 [5]	0.56±0.07 [5]	0.66±0.11 [4]	0.79±0.13 [6]

Values (institutional units) are given as mean ± standard deviation [n]. MRS, magnetic resonance spectroscopy; NAA, N-acetyl aspartate; Cr, creatine; Cho, choline; Ins, myo-inositol; Glu, glutamate; Gln, glutamine.

DTI measurements

The mean diffusivity of the left hippocampus showed significant group (P=8.21e-05), sex (P=0.000454), litter (P=7.68e-05), and sex-by-litter (P=0.000272) effects. However, post-hoc t-tests comparing each group and males to females showed no significant differences.

Discussion

Volume changes have been reported in the CLS study with brain volume decreases generally associated with higher childhood blood lead levels (12). Whereas the CLS study found volume deficits in frontal gray matter (12), we found no significant volumetric differences.

The CLS study also demonstrated an inverse relationship between mean childhood blood lead level and metabolite concentrations in various brain regions, including the basal ganglia and frontal and parietal white matter (15). The majority of changes were found in white matter, which was not examined here due to the small white matter volumes in mice.
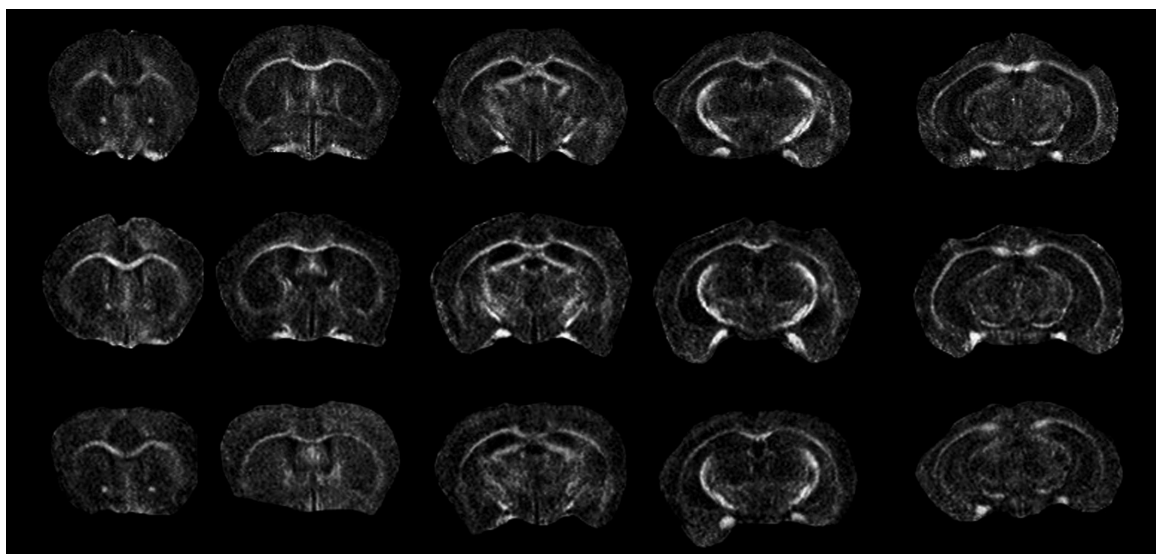
Figure 2 Fractional anisotropy maps derived from diffusion tensor imaging echo planar imaging acquired with TR/TE 5,400/40 ms, 4 shots, 4 repetitions, 30 directions at a b-value of 670, 75 μm in-plane resolution, matrix 196×168, and 700 μm slice thickness. Each row illustrates five selected images from three different mice.

Table 4 Diffusion tensor imaging (DTI) results

Region of interest by exposure group	Female				Male			
	RD	MD*	AD	FA	RD	MD*	AD	FA
Left hippocampus								
0 ppm	0.63±0.03 [5]	2.44±0.07 [5]	1.18±0.01 [5]	0.40±0.03 [5]	0.67±0.06 [9]	2.57±0.17 [9]	1.22±0.06 [9]	0.38±0.03 [9]
3 ppm	0.66±0.02 [9]	2.49±0.06 [9]	1.17±0.05 [9]	0.37±0.03 [9]	0.68±0.04 [5]	2.55±0.10 [5]	1.20±0.10 [5]	0.36±0.07 [5]
30 ppm	0.75±0.20 [8]	2.59±0.17 [8]	1.20±0.07 [8]	0.35±0.04 [8]	0.70±0.06 [10]	2.64±0.17 [10]	1.23±0.07 [10]	0.36±0.03 [10]
Right hippocampus								
0 ppm	0.68±0.02 [5]	2.56±0.04 [5]	1.20±0.04 [5]	0.36±0.03 [5]	0.69±0.06 [8]	2.63±0.16 [8]	1.26±0.07 [8]	0.38±0.04 [8]
3 ppm	0.70±0.03 [9]	2.58±0.10 [9]	1.18±0.06 [9]	0.35±0.03 [9]	0.70±0.06 [6]	2.64±0.15 [6]	1.24±0.13 [6]	0.36±0.10 [6]
30 ppm	0.77±0.19 [7]	2.57±0.09 [7]	1.19±0.04 [7]	0.35±0.03 [7]	0.74±0.05 [7]	2.74±0.15 [7]	1.25±0.05 [7]	0.34±0.02 [7]

Values are given as mean ± standard deviation [n] for fractional anisotropy (FA) or (mean ×1,000) ± standard deviation [n] for radial diffusivity (RD), mean diffusivity (MD), and axial diffusivity (AD). *Effects of group ($P=8.21e-05$), sex ($P=0.000454$), litter ($P=7.68e-05$), and sex-by-litter ($P=0.000272$) were significant.

In frontal cortex, no significant lead-related metabolic changes were found in either the CLS study or the current study.

Sex-related effects have not been found consistently in MRS data. Sex-related effects have been found in a mouse study of Alzheimer's (28), but do not appear to have been examined in any other study. We found sex effects in thalamus only for glutamate and the glutamate/glutamine complex signal.

Analysis of DTI data from the CLS cohort revealed diffuse alterations in white matter (14). Mice have less white matter than humans, making direct comparison of the results difficult. Both studies examined corpus callosum and internal capsule. Significant effects of lead were found in these regions in the CLS cohort (14), but not in the mice. This may be due to partial volume effects in the mice masking changes in the DTI parameters. In general, the mice results show no significant sex or exposure effects for the DTI measurements anywhere except in the

hippocampus, a region not examined in the CLS study. Sex effects in rodents have not been reported for these DTI measurements to our knowledge, but are well-known in humans [see Sacher *et al.* (29) for a review]. Our data suggest that sex may influence hippocampal structure in mice, but further work needs to be done at higher resolution focusing on this question.

The lead doses we used may have been too small to cause measureable changes in the MRI data. The two prior rodent studies in which imaging alterations were reported used significantly higher lead doses (500 ppm in the study by López-Larrubia (19) and over 1,000 ppm in the study by Meng (17) compared with the maximum value of 30 ppm herein). The minimal changes found in our DTI are consistent with the negative results reported by López-Larrubia (19) for a 50 ppm exposure over 4 weeks. Only after a 12-week exposure to 50 ppm lead acetate did the reported apparent diffusion coefficient values differ significantly from controls in these adult animals.

This study evaluated the effects of pre- and perinatal lead exposure on neuroimaging markers in adult mouse brain. This model does not explain the findings from the CLS, since minimal changes were found. Parsing the role of lead on brain development in human subjects is difficult due to the many complexities of human exposure, including cumulative dose over childhood and into adulthood, timing of exposure, ongoing myelination and development of various brain structures, as well as the role of ongoing exposure due to leaching during bone growth, pregnancy, etc. A sensitive animal model would be useful to distinguish these different factors. The results of this study suggest that this animal model is not sufficiently sensitive to demonstrate the effects of lead exposure on imaging.

Acknowledgements

Footnote

Conflicts of Interest: The authors have no conflicts of interest to declare.

References

1. Bhattacharya A, Shukla R, Dietrich KN, Bornschein RL. Effect of early lead exposure on the maturation of children's postural balance: a longitudinal study. Neurotoxicol Teratol 2006;28:376-85.

2. Chen A, Dietrich KN, Ware JH, Radcliffe J, Rogan WJ. IQ and blood lead from 2 to 7 years of age: are the effects in older children the residual of high blood lead concentrations in 2-year-olds? Environ Health Perspect 2005;113:597-601.

3. Dietrich KN, Berger OG, Succop PA. Lead exposure and the motor developmental status of urban six-year-old children in the Cincinnati Prospective Study. Pediatrics 1993;91:301-7.

4. Dietrich KN, Berger OG, Succop PA, Hammond PB, Bornschein RL. The developmental consequences of low to moderate prenatal and postnatal lead exposure: intellectual attainment in the Cincinnati Lead Study Cohort following school entry. Neurotoxicol Teratol 1993;15:37-44.

5. Dietrich KN, Ris MD, Succop PA, Berger OG, Bornschein RL. Early exposure to lead and juvenile delinquency. Neurotoxicol Teratol 2001;23:511-8.

6. Hornung RW, Lanphear BP, Dietrich KN. Age of greatest susceptibility to childhood lead exposure: a new statistical approach. Environ Health Perspect 2009;117:1309-12.

7. Lanphear BP, Hornung R, Khoury J, Yolton K, Baghurst P, Bellinger DC, Canfield RL, Dietrich KN, Bornschein R, Greene T, Rothenberg SJ, Needleman HL, Schnaas L, Wasserman G, Graziano J, Roberts R. Low-level environmental lead exposure and children's intellectual function: an international pooled analysis. Environ Health Perspect 2005;113:894-9.

8. Baghurst PA, McMichael AJ, Wigg NR, Vimpani GV, Robertson EF, Roberts RJ, Tong SL. Environmental exposure to lead and children's intelligence at the age of seven years. The Port Pirie Cohort Study. N Engl J Med 1992;327:1279-84.

9. Bellinger DC, Stiles KM, Needleman HL. Low-level lead exposure, intelligence and academic achievement: a long-term follow-up study. Pediatrics 1992;90:855-61.

10. Canfield RL, Henderson CR Jr, Cory-Slechta DA, Cox C, Jusko TA, Lanphear BP. Intellectual impairment in children with blood lead concentrations below 10 microg per deciliter. N Engl J Med 2003;348:1517-26.

11. Wasserman GA, Liu X, Lolacono NJ, Factor-Litvak P, Kline JK, Popovac D, Morina N, Musabegovic A, Vrenezi N, Capuni-Paracka S, Lekic V, Preteni-Redjepi

E, Hadzialjevic S, Slavkovich V, Graziano JH. Lead exposure and intelligence in 7-year-old children: the Yugoslavia Prospective Study. Environ Health Perspect 1997;105:956-62.

12. Cecil KM, Brubaker CJ, Adler CM, Dietrich KN, Altaye M, Egelhoff JC, Wessel S, Elangovan I, Hornung R, Jarvis K, Lanphear BP. Decreased brain volume in adults with childhood lead exposure. PLoS Med 2008;5:e112.

13. Stewart WF, Schwartz BS, Davatzikos C, Shen D, Liu D, Wu X, Todd AC, Shi W, Bassett S, Youssem D. Past adult lead exposure is linked to neurodegeneration measured by brain MRI. Neurology 2006;66:1476-84.

14. Brubaker CJ, Schmithorst VJ, Haynes EN, Dietrich KN, Egelhoff JC, Lindquist DM, Lanphear BP, Cecil KM. Altered myelination and axonal integrity in adults with childhood lead exposure: a diffusion tensor imaging study. Neurotoxicology 2009;30:867-75.

15. Cecil KM, Dietrich KN, Altaye M, Egelhoff JC, Lindquist DM, Brubaker CJ, Lanphear BP. Proton magnetic resonance spectroscopy in adults with childhood lead exposure. Environ Health Perspect 2011;119:403-8.

16. Yamazaki Y, Mann MR, Lee SS, Marh J, McCarrey JR, Yanagimachi R, Bartolomei MS. Reprogramming of primordial germ cells begins before migration into the genital ridge, making these cells inadequate donors for reproductive cloning. Proc Natl Acad Sci U S A 2003;100:12207-12.

17. Meng XM, Ruan DY, Kang LD, Zhu DM, She JQ, Luo L, Zheng Y, Li XH. Age-related morphological impairments in the rat hippocampus following developmental lead exposure: an MRI, LM and EM study. Environ Toxicol Pharmacol 2003;13:187-97.

18. Baranowska-Bosiacka I, Strużyńska L, Gutowska I, Machalińska A, Kolasa A, Kłos P, Czapski GA, Kurzawski M, Prokopowicz A, Marchlewicz M, Safranow K, Machaliński B, Wiszniewska B, Chlubek D. Perinatal exposure to lead induces morphological, ultrastructural and molecular alterations in the hippocampus. Toxicology 2013;303:187-200.

19. López-Larrubia P, Cauli O. Alterations of apparent diffusion coefficient (ADC) in the brain of rats chronically exposed to lead acetate. Toxicology 2011;281:1-6.

20. Sánchez-Martín FJ, Lindquist DM, Landero-Figueroa J, Zhang X, Chen J, Cecil KM, Medvedovic M, Puga A. Sex- and tissue-specific methylome changes in brains of mice perinatally exposed to lead. Neurotoxicology 2015;46:92-100.

21. Schneider CA, Rasband WS, Eliceiri KW. NIH Image to ImageJ: 25 years of image analysis. Nat Methods 2012;9:671-5.

22. Biedermann S, Fuss J, Zheng L, Sartorius A, Falfán-Melgoza C, Demirakca T, Gass P, Ende G, Weber-Fahr W. In vivo voxel based morphometry: detection of increased hippocampal volume and decreased glutamate levels in exercising mice. Neuroimage 2012;61:1206-12.

23. Provencher SW. Estimation of metabolite concentrations from localized in vivo proton NMR spectra. Magn Reson Med 1993;30:672-9.

24. Jiang H, van Zijl PC, Kim J, Pearlson GD, Mori S. DtiStudio: resource program for diffusion tensor computation and fiber bundle tracking. Comput Methods Programs Biomed 2006;81:106-16.

25. Ercal N, Treeratphan P, Hammond TC, Matthews RH, Grannemann NH, Spitz DR. In vivo indices of oxidative stress in lead-exposed C57BL/6 mice are reduced by treatment with meso-2,3-dimercaptosuccinic acid or N-acetylcysteine. Free Radic Biol Med 1996;21:157-61.

26. Iavicoli I, Carelli G, Stanek EJ, Castellino N, Calabrese EJ. Effects of low doses of dietary lead on red blood cell production in male and female mice. Toxicol Lett 2003;137:193-9.

27. Virgolini MB, Rossi-George A, Weston D, Cory-Slechta DA. Influence of low level maternal Pb exposure and prenatal stress on offspring stress challenge responsivity. Neurotoxicology 2008;29:928-39.

28. van Duijn S, Nabuurs RJ, van Duinen SG, Natté R, van Buchem MA, Alia A. Longitudinal monitoring of sex-related in vivo metabolic changes in the brain of Alzheimer's disease transgenic mouse using magnetic resonance spectroscopy. J Alzheimers Dis 2013;34:1051-9.

29. Sacher J, Neumann J, Okon-Singer H, Gotowiec S, Villringer A. Sexual dimorphism in the human brain: evidence from neuroimaging. Magn Reson Imaging 2013;31:366-75.